

## Research



**Cite this article:** Holzapfel GA, Ogden RW. 2020 A damage model for collagen fibres with an application to collagenous soft tissues. *Proc. R. Soc. A* **476**: 20190821. <http://dx.doi.org/10.1098/rspa.2019.0821>

Received: 26 November 2019

Accepted: 19 March 2020

**Subject Areas:**

biomechanics

**Keywords:**

artery elasticity, collagen fibres, collagen cross-links, fibrous tissue, fibre damage

**Author for correspondence:**

Gerhard A. Holzapfel

e-mail: [holzapfel@tugraz.at](mailto:holzapfel@tugraz.at)

# A damage model for collagen fibres with an application to collagenous soft tissues

Gerhard A. Holzapfel<sup>1,2</sup> and Ray W. Ogden<sup>3</sup>

<sup>1</sup>Institute of Biomechanics, Graz University of Technology, Stremayrgasse 16-II, 8010 Graz, Austria

<sup>2</sup>Norwegian University of Science and Technology (NTNU), Faculty of Engineering Science and Technology, 7491 Trondheim, Norway

<sup>3</sup>School of Mathematics and Statistics, University of Glasgow, University Place, Glasgow G12 8SQ, UK

GAH, 0000-0001-8119-5775; RWO, 0000-0002-7002-7028

We propose a mechanical model to account for progressive damage in collagen fibres within fibrous soft tissues. The model has a similar basis to the pseudoelastic model that describes the Mullins effect in rubber but it also accounts for the effect of cross-links between collagen fibres. We show that the model is able to capture experimental data obtained from rat tail tendon fibres, and the combined effect of damage and collagen cross-links is illustrated for a simple shear test. The proposed three-dimensional framework allows a straightforward implementation in finite-element codes, which are needed to analyse more complex boundary-value problems for soft tissues under supra-physiological loading or tissues weakened by disease.

## 1. Introduction

Fibrous soft tissues consist of distributions of collagen fibres which, for example, could be almost parallel, as is the case for tendons, dispersed, as for artery walls, or isotropic, as for the middle zone of cartilage. These fibres are embedded in an essentially isotropic extracellular matrix consisting of elastic fibres (including elastin), proteoglycans, water, adhesion proteins and integrins, *inter alia*. Of particular interest are the mechanical properties of the collagen fibres, the main load-bearing constituents of soft tissues, and their contribution to the overall behaviour of the tissues [1]. There are several constitutive models available that capture the distribution of collagen fibres [2–5]. However, it is

important to note that under certain supra-physiological loads and in certain tissue diseases collagen starts to soften and finally ruptures, as shown by the experimental data in Pins & Silver [6] on a single collagen fibre. But as yet such effects on the microscale have not been incorporated in constitutive models. For soft biological tissues, a number of damage models are available, as described in [7]. For example, one study [8] derives a fibre/fibril damage model based on failure once a critical tissue stretch is reached. The proposed model reproduces the typical nonlinear behaviour of ligaments, including the toe and linear regions, then damage and eventual failure. The computational work in [9] proposes a (rather complex) macroscopic tissue damage model by considering recruitment stretches for the fibre content and failure of fibres in a distribution at different stretches or strain energies. Decoupled damage mechanisms for the matrix and fibres are considered. On the basis of [8], the constitutive model in [10] considers fibre recruitment and damage distributions by using probability density functions. It also includes a constitutive model for unloading after damage. The work in [11] applies the constrained mixture theory of [12] to study the formation/dilatation of abdominal aortic aneurysms. In particular, the constitutive model accounts for continuous degradation and creation of collagen fibres (i.e. the disappearance of old collagen and appearance of new collagen). The purpose of the present paper is now to develop a basic model at the collagen/cross-link microscale level that can account for these softening and failure effects.

The influence of the concentration of collagen fibre cross-links on the anisotropic response of fibrous soft tissues such as arterial walls was first analysed with a fully three-dimensional model in [13]. However, that approach was solely based on the theory of hyperelasticity and no damage mechanism was included, which limits its applicability. Another aim of this paper is, therefore, to account for collagen fibre damage in the presence of undamaged cross-links, which is the subject of §2. The model has a similar structure to that of the pseudoelastic model of the Mullins effect of rubber published in [14] but takes account of damage during loading rather than unloading. In the present account, this damage model is used to reproduce the experimental behaviour of rat tail tendon fibres. In §3, with the inclusion of cross-links, we analyse the combined effect of damage and cross-links in the simple shear of a single family of parallel fibres embedded in an isotropic matrix. In particular, we demonstrate the influence of damage and the proportion of cross-links on the shear stress versus the amount of shear response. This illustrates that fibre damage leads to a softening behaviour and finally failure of the tissue. In §4, we provide concluding remarks and point to the needs for further experimental data at the microscopic level to inform the macroscopic tissue behaviour. This model approach can be implemented in a finite-element code to execute more realistic boundary-value problems, for which purpose we provide the elasticity tensor in appendix A.

## 2. Damage model considering cross-linking

### (a) Damage formulation

We start by introducing the deformation gradient  $\mathbf{F}$  relative to a given reference configuration, and the related right and left Cauchy–Green tensors  $\mathbf{C} = \mathbf{F}^T \mathbf{F}$  and  $\mathbf{b} = \mathbf{F} \mathbf{F}^T$ , respectively. For further use, we define the isotropic invariant  $I_1$  and the pseudo-invariant  $I_4$  according to

$$I_1 = \text{tr } \mathbf{C} \quad \text{and} \quad I_4 = (\mathbf{C}\mathbf{M}) \cdot \mathbf{M} = \lambda^2, \quad (2.1)$$

where  $\mathbf{M}$  is the direction of aligned fibres in the stress-free reference configuration which are embedded in an isotropic matrix and  $\lambda$  is the fibre stretch. Now let us consider a fibre-reinforced material such as a collagenous soft tissue, which is subject to the incompressibility constraint  $\det \mathbf{F} = 1$ , with a strain-energy function of the form  $\Psi(I_1, I_4)$ . The Cauchy stress tensor  $\boldsymbol{\sigma}$  is then given by [15]

$$\boldsymbol{\sigma} = 2\psi_1 \mathbf{b} + 2\psi_4 \mathbf{m} \otimes \mathbf{m} - p\mathbf{I}, \quad (2.2)$$

where  $p$  is a Lagrange multiplier and  $\mathbf{m} = \overline{\mathbf{FM}}$  is the fibre direction in the deformed configuration. Here, for convenience, we have introduced the abbreviations

$$\psi_1 = \frac{\partial \Psi}{\partial I_1} \quad \text{and} \quad \psi_4 = \frac{\partial \Psi}{\partial I_4}. \quad (2.3)$$

Now we consider the possibility of damage occurring when the stretch  $\lambda$  in the fibre exceeds some critical value, say  $\lambda_c$ . To model the damage effect, we introduce a (dimensionless) damage variable  $\eta$ , which is an additional independent variable so that  $\Psi(I_1, I_4, \eta)$ . In the damage phase, the Cauchy stress is again given by (2.2) with the optimization condition

$$\frac{\partial \Psi}{\partial \eta} = 0, \quad (2.4)$$

which gives  $\eta$  implicitly in terms of  $I_1$  and  $I_4$ . Let  $I_{4c} = \lambda_c^2$  be the critical value of  $I_4$ . We take  $\eta = 1$  whenever  $I_4 \leq I_{4c}$ , so (2.2) applies with  $\Psi(I_1, I_4, 1)$  and (2.4) is not active. For definiteness, we now take

$$\Psi(I_1, I_4, \eta) = \Psi_{\text{iso}}(I_1) + \eta \Psi_{\text{fib}}(I_4) + \phi(\eta), \quad (2.5)$$

analogously to the model of the Mullins effect [14], where  $\phi(\eta)$  is some measure of damage. Then (2.2) gives

$$\boldsymbol{\sigma} = 2\psi_1 \mathbf{b} + 2\eta \psi_f \mathbf{m} \otimes \mathbf{m} - p \mathbf{I}, \quad (2.6)$$

where we have introduced the abbreviations

$$\psi_1 = \frac{\partial \Psi_{\text{iso}}}{\partial I_1} \quad \text{and} \quad \psi_f = \frac{\partial \Psi_{\text{fib}}}{\partial I_4}, \quad (2.7)$$

and with (2.5) the optimization condition (2.4) gives

$$\phi'(\eta) = -\Psi_{\text{fib}}(I_4), \quad (2.8)$$

which determines  $\eta$  in terms of  $I_4$ , i.e. damage is only related to the fibres. We require

$$\phi(1) = 0 \quad \text{and} \quad \phi'(1) = -\Psi_{\text{fib}}(I_{4c}). \quad (2.9)$$

Note that if we use (2.4) to give  $\eta = \eta(I_4)$  and write, say,

$$\overline{\Psi}(I_4) = \eta \Psi_{\text{fib}}(I_4) + \phi(\eta), \quad (2.10)$$

then by (2.8) we obtain  $\overline{\Psi}' = \eta \psi_f$ , where  $\psi_f$  is according to (2.7)<sub>2</sub>. This leads to an alternative arrival at the second term on the right-hand side of (2.6).

A suitable choice of  $\phi'(\eta)$ , which gives a decaying behaviour for  $\eta$  as  $I_4$  increases beyond  $I_{4c}$  and damage progresses, is

$$\phi'(\eta) = m \log \eta - \Psi_{\text{fib}}(I_{4c}), \quad (2.11)$$

and hence, by (2.8),

$$\eta = \exp\left(-\frac{\Psi_{\text{fib}}(I_4) - \Psi_{\text{fib}}(I_{4c})}{m}\right), \quad (2.12)$$

where  $m > 0$  is a parameter with the same dimension as  $\Psi$ . Figure 1 provides a schematic of the damage parameter  $\eta$  as a function of the stretch  $\lambda$ . It shows that  $\eta$  decreases from 1 when the stretch  $\lambda$  increases beyond the critical value  $\lambda_c$  down to the value  $\eta_f$  when  $\lambda$  reaches the failure value  $\lambda_f$ . This schematic is based on specific calculations of  $\eta$  for uniaxial extension and simple shear, which exhibit very similar behaviour.

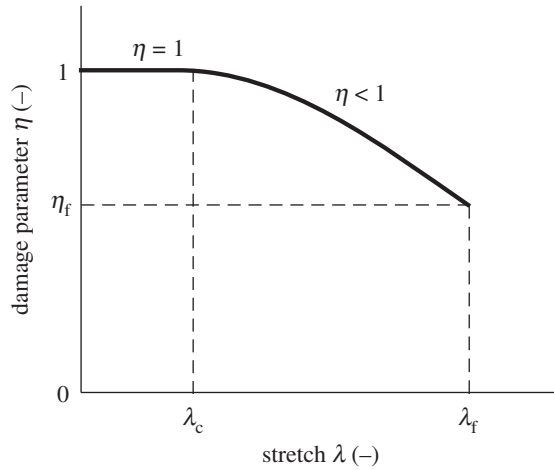


**Figure 1.** Damage parameter  $\eta$  versus stretch  $\lambda$ , with critical stretch  $\lambda_c$  and failure stretch  $\lambda_f$ .

### (b) Uniaxial extension

Let  $\lambda$  be the stretch in the fibre direction  $\mathbf{M}$  and  $\sigma$  the related uniaxial Cauchy stress. Then, the components of (2.6) yield

$$\sigma = 2\psi_i\lambda^2 + 2\eta\lambda^2\psi_f - p \quad \text{and} \quad 0 = 2\psi_i\lambda^{-1} - p, \quad (2.13)$$

and hence, on elimination of  $p$ ,

$$\sigma = 2\psi_i(\lambda^2 - \lambda^{-1}) + 2\eta\lambda^2\psi_f, \quad (2.14)$$

where  $\psi_i$  and  $\psi_f$  are defined in (2.7). Now choose

$$\Psi_{\text{iso}} = \frac{\mu}{2}(I_4 - 3) \quad \text{and} \quad \Psi_{\text{fib}} = \frac{k_1}{2k_2} \left\{ \exp[k_2(I_4 - 1)^2] - 1 \right\}, \quad (2.15)$$

for the matrix and the fibre properties, respectively, where  $\mu$  and  $k_1$  are stress-like parameters, while  $k_2$  is dimensionless. Hence, according to (2.7),  $2\psi_i = \mu$  and  $2\psi_f = 2k_1(I_4 - 1) \exp[k_2(I_4 - 1)^2]$ , so that (2.12), gives

$$\eta = \exp \left[ -\frac{k_1}{2mk_2} \left\{ \exp[k_2(I_4 - 1)^2] - \exp[k_2(I_{4c} - 1)^2] \right\} \right], \quad (2.16)$$

with  $I_4 = \lambda^2$  and  $I_{4c} = \lambda_c^2$ .

From (2.14), we then obtain

$$\sigma = \mu(\lambda^2 - \lambda^{-1}) + 2k_1\lambda^2(\lambda^2 - 1) \exp[k_2(\lambda^2 - 1)^2], \quad (2.17)$$

when no damage occurs ( $\lambda \leq \lambda_c$ ), and

$$\sigma = \mu(\lambda^2 - \lambda^{-1}) + 2\eta k_1\lambda^2(\lambda^2 - 1) \exp[k_2(\lambda^2 - 1)^2], \quad (2.18)$$

with (2.16), when  $\lambda \geq \lambda_c$ .

The nominal stress  $P = \sigma/\lambda$  is plotted in figure 2 as a fit to the uniaxial test data from a rat tail tendon fibre shown in [6], using the parameter values  $\mu = 0$ ,  $k_1 = 115$  MPa,  $k_2 = 7.7$ ,  $m = 6$  MPa and  $\lambda_c = 1.05$ . Note that, since we are modelling a single fibre here, we emphasize that there is no need to include the isotropic term.

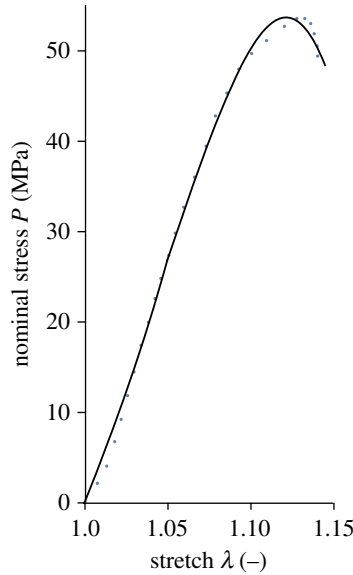


**Figure 2.** Fit to experimental data from a rat tail tendon fibre taken from [6], whereby the dots represent the data extracted digitally from the curve in [6]. The solid curve shows the nominal stress  $P = \sigma/\lambda$  versus stretch  $\lambda$  according to (2.18) with  $\mu = 0$  and  $k_1 = 115$  MPa,  $k_2 = 7.7$ ,  $m = 6$  MPa,  $\lambda_c = 1.05$ .

From (2.9)<sub>1</sub> and (2.11), we have

$$\phi(\eta) = m\eta \log \eta + (1 - \eta)[m + \Psi_{\text{fib}}(I_{4c})], \quad (2.19)$$

and from (2.12)

$$m \log \eta = \Psi_{\text{fib}}(I_{4c}) - \Psi_{\text{fib}}(I_4). \quad (2.20)$$

There is no energy loss for  $I_4 \leq I_{4c}$ . Energy loss for  $I_4 \geq I_{4c}$  is given by

$$\Psi_{\text{fib}} - [\eta\Psi_{\text{fib}} + \phi(\eta)] = m(\eta - \log \eta - 1) > 0 \quad \text{for } \eta < 1. \quad (2.21)$$

Although there are no data available for the unloading phase, it is worthwhile illustrating the stress softening effect induced by  $\eta$  during unloading prior to failure. For uniaxial extension, this is shown by the schematic in figure 3 with three unloading curves from different points on the loading path. This parallels figure 2 with the nominal stress versus stretch.

### (c) Inclusion of collagen fibre cross-links

Let us use the unit vector  $\mathbf{M}$ , which identifies the collagen fibre direction in the reference configuration, and introduce  $\mathbf{N}$ , which is an arbitrary unit vector orthogonal to  $\mathbf{M}$ . Now we consider two families of cross-links around the collagen fibre direction  $\mathbf{M}$  with the unit vectors  $\mathbf{L}^+$  and  $\mathbf{L}^-$ , which are rotationally symmetric about  $\mathbf{M}$ , and with the action of  $\mathbf{F}$  on them defined by

$$\mathbf{L}^\pm = \pm \cos \alpha_0 \mathbf{M} + \sin \alpha_0 \mathbf{N} \quad \text{and} \quad \mathbf{F}\mathbf{L}^\pm = \pm c_0 \mathbf{F}\mathbf{M} + s_0 \mathbf{F}\mathbf{N}, \quad (2.22)$$

where  $\alpha_0$  defines their orientation relative to the direction  $\mathbf{M}$  (figure 4). For conciseness, we have written  $s_0 = \sin \alpha_0$  and  $c_0 = \cos \alpha_0$ .

The invariant  $I_4$  associated with the fibre direction is given in (2.1)<sub>2</sub>, and the invariants  $I^\pm$ , which are the squares of the stretches in the cross-link directions, and the quantities  $I_8^\pm$  describing

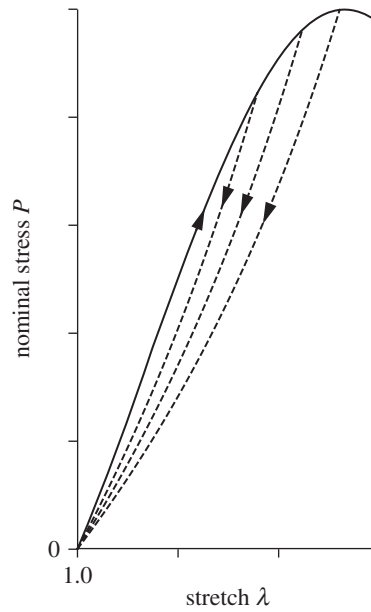


**Figure 3.** Schematic of the nominal stress  $P$  versus stretch  $\lambda$  during loading in uniaxial extension (continuous curve), with unloading curves (dashed) from three different points on the loading curve prior to failure.

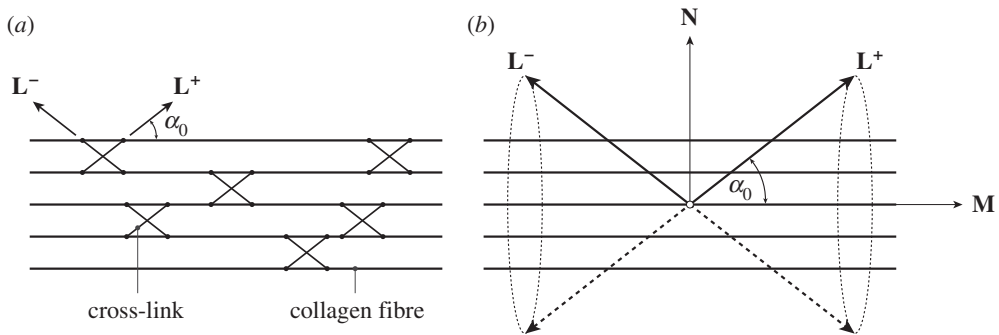


**Figure 4.** (a) Parallel fibres in the  $M$  direction with two families of parallel cross-links described by the vectors  $L^+$  and  $L^-$  making an angle  $\alpha_0$  with  $M$ . (b) Detail of a pair of cross-links, showing rotational symmetry about the  $M$  direction with the orthogonal vector  $N$  (modified from [13]).

the coupling between the collagen fibres and cross-links are defined by Holzapfel & Ogden [13]

$$I^\pm = c_0^2 I_4 \pm 2s_0 c_0 (\mathbf{CM}) \cdot \mathbf{N} + s_0^2 (\mathbf{CN}) \cdot \mathbf{N} \quad \text{and} \quad I_8^\pm = \pm c_0 I_4 + s_0 (\mathbf{CM}) \cdot \mathbf{N}. \quad (2.23)$$

Note that, in general,  $I^+ \neq I^-$  and  $I_8^+ \neq -I_8^-$ .

From the derivatives of  $I_4$ ,  $I^\pm$  and  $I_8^\pm$  with respect to the right Cauchy–Green tensor  $\mathbf{C}$  given in [13] applied to a strain-energy function  $\Psi(I_1, I_4, I^+, I^-, I_8^+, I_8^-)$ , we obtain the general expression of

the Cauchy stress tensor as

$$\begin{aligned} \boldsymbol{\sigma} = & -p\mathbf{I} + 2\psi_1\mathbf{b} + 2\psi_4\mathbf{FM} \otimes \mathbf{FM} \\ & + 2\psi_{I^+}[c_0^2\mathbf{FM} \otimes \mathbf{FM} + s_0c_0(\mathbf{FM} \otimes \mathbf{FN} + \mathbf{FN} \otimes \mathbf{FM}) + s_0^2\mathbf{FN} \otimes \mathbf{FN}] \\ & + 2\psi_{I^-}[c_0^2\mathbf{FM} \otimes \mathbf{FM} - s_0c_0(\mathbf{FM} \otimes \mathbf{FN} + \mathbf{FN} \otimes \mathbf{FM}) + s_0^2\mathbf{FN} \otimes \mathbf{FN}] \\ & + \psi_{8^+}[2c_0\mathbf{FM} \otimes \mathbf{FM} + s_0(\mathbf{FM} \otimes \mathbf{FN} + \mathbf{FN} \otimes \mathbf{FM})] \\ & + \psi_{8^-}[-2c_0\mathbf{FM} \otimes \mathbf{FM} + s_0(\mathbf{FM} \otimes \mathbf{FN} + \mathbf{FN} \otimes \mathbf{FM})], \end{aligned} \quad (2.24)$$

as in [13], but with a slightly different notation, where we have used the abbreviations

$$\psi_{I^\pm} = \frac{\partial \Psi}{\partial I^\pm} \quad \text{and} \quad \psi_{8^\pm} = \frac{\partial \Psi}{\partial I_8^\pm} \quad (2.25)$$

in addition to  $\psi_1$  and  $\psi_4$  defined in (2.3).

Note that the second Piola–Kirchhoff stress, which is important for finite-element implementations, here denoted by  $\mathbf{S}$ , is related to  $\boldsymbol{\sigma}$  by  $\mathbf{S} = \mathbf{F}^{-1}\boldsymbol{\sigma}\mathbf{F}^{-T}$  for an incompressible material. Consequently, we can determine the total differential

$$d\mathbf{S} = \mathbb{C} : \frac{1}{2}d\mathbf{C}, \quad (2.26)$$

where the colon denotes the standard double contraction and  $\mathbb{C}$  is the elasticity tensor in the material description required for finite-element analysis. For a general explicit expression for  $\mathbb{C}$ , we refer to appendix A.

### (i) Uniaxial extension with cross-linking

For uniaxial extension with stretch  $\lambda$  in the fibre direction, we have

$$\mathbf{FM} = \lambda\mathbf{M} \quad \text{and} \quad \mathbf{FN} = \lambda^{-1/2}\mathbf{N}. \quad (2.27)$$

Hence, with these two equations we can deduce from (2.22)<sub>2</sub>

$$\mathbf{FL}^\pm = \pm c_0\lambda\mathbf{M} + s_0\lambda^{-1/2}\mathbf{N}, \quad (2.28)$$

and (2.23) specializes to

$$I \equiv I^\pm = c_0^2\lambda^2 + s_0^2\lambda^{-1}, \quad I_8 = I_8^+ = c_0\lambda^2 \quad \text{and} \quad I_8^- = -I_8^+. \quad (2.29)$$

Then  $\psi_I = \psi_{I^+} = \psi_{I^-}$ ,  $\psi_{8^+} = -\psi_{8^-} = \psi_8$ , and (2.24) specializes to

$$\begin{aligned} \boldsymbol{\sigma} = & -p\mathbf{I} + 2\psi_1(\lambda^2\mathbf{M} \otimes \mathbf{M} + \lambda^{-1}\mathbf{N} \otimes \mathbf{N}) + 2\psi_4\lambda^2\mathbf{M} \otimes \mathbf{M} \\ & + 4\psi_I(c_0^2\lambda^2\mathbf{M} \otimes \mathbf{M} + s_0^2\lambda^{-1}\mathbf{N} \otimes \mathbf{N}) + 4\psi_8c_0\lambda^2\mathbf{M} \otimes \mathbf{M}, \end{aligned} \quad (2.30)$$

the relevant components of which are

$$\sigma = -p + 2\psi_1\lambda^2 + 2\psi_4\lambda^2 + 4\psi_Ic_0^2\lambda^2 + 4\psi_8c_0\lambda^2 \quad (2.31)$$

and

$$0 = -p + 2\psi_1\lambda^{-1} + 4\psi_I s_0^2\lambda^{-1}. \quad (2.32)$$

By eliminating the Lagrange multiplier  $p$  we obtain

$$\sigma = 2\psi_1(\lambda^2 - \lambda^{-1}) + 2\psi_4\lambda^2 + 4\psi_I(c_0^2\lambda^2 - s_0^2\lambda^{-1}) + 4\psi_8c_0\lambda^2. \quad (2.33)$$

Now let us use the specific strain-energy functions (2.15) supplemented by quadratic energy functions associated with the cross-links and fibre/cross-link interactions so that

$$\Psi = \frac{1}{2}\mu(I_1 - 3) + \eta \frac{k_1}{2k_2} \{ \exp[k_2(I_4 - 1)^2] - 1 \} + \frac{1}{2}\nu(I - 1)^2 + \frac{1}{2}\kappa(I_8 - c_0)^2, \quad (2.34)$$

where  $\nu$  and  $\kappa$  are parameters with dimension of stress associated with the cross-links and interactions, respectively. In particular, a larger  $\nu$  corresponds to a larger density of cross-links,

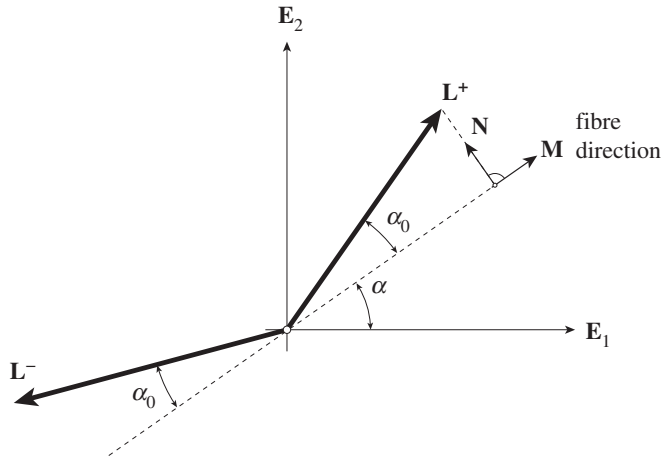


**Figure 5.**  $\mathbf{M}$  represents the direction of a family of aligned fibres with unit normal  $\mathbf{N}$  with respect to background axes  $\mathbf{E}_1$  and  $\mathbf{E}_2$ , and  $\mathbf{M}$  makes an angle  $\alpha$  with respect to the  $\mathbf{E}_1$  direction.  $\mathbf{L}^\pm$  represents the directions of two families of cross-links, and  $\mathbf{L}^\pm$  make an angle  $\alpha_0$  with respect to the  $\pm\mathbf{M}$  direction (modified from Holzapfel & Ogden [13]).

while  $\kappa$  is a measure of the interaction energy. Here, we have adopted very simple models for the energy in the cross-links and the interaction energy since there are no data available to justify more sophisticated forms of energy. From (2.12) with (2.15)<sub>2</sub>,  $\eta$  is given by

$$\eta = \exp \left[ -\frac{k_1}{2mk_2} \left\{ \exp[k_2(\lambda^2 - 1)^2] - \exp[k_2(\lambda_c^2 - 1)^2] \right\} \right]. \quad (2.35)$$

From (2.33) to (2.34), with the help of (2.3) and (2.25), the Cauchy stress  $\sigma$  then becomes

$$\begin{aligned} \sigma = & \mu(\lambda^2 - \lambda^{-1}) + 2k_1\eta\lambda^2(\lambda^2 - 1)\exp[k_2(\lambda^2 - 1)^2] \\ & + 4\nu(I - 1)(c_0^2\lambda^2 - s_0^2\lambda^{-1}) + 4\kappa(I_8 - c_0)c_0\lambda^2. \end{aligned} \quad (2.36)$$

The fit to the experimental data of [6] is of similar agreement to that shown in figure 2. Specific parameters are, for example,  $k_1 = 120$  MPa,  $\nu = 15$  MPa,  $k_2 = 6.4$ ,  $m = 6$  MPa,  $\alpha_0 = \pi/4$ ,  $\lambda_c = 1.02$ ,  $\kappa = 8$  MPa and  $\mu = 0$ .

### 3. Application to planar deformation of soft tissues

Next, we consider the situation in which the collagen fibres and cross-links are restricted to the  $(\mathbf{E}_1, \mathbf{E}_2)$  plane and we define by  $\mathbf{M}$  the direction of the family of aligned fibres and its normal  $\mathbf{N}$  as

$$\mathbf{M} = \cos \alpha \mathbf{E}_1 + \sin \alpha \mathbf{E}_2 \quad \text{and} \quad \mathbf{N} = -\sin \alpha \mathbf{E}_1 + \cos \alpha \mathbf{E}_2, \quad (3.1)$$

where  $\alpha$  is the angle between the fibre direction and the  $\mathbf{E}_1$  axis (figure 5). With respect to  $\mathbf{M}$  and  $\mathbf{N}$  the cross-link directions  $\mathbf{L}^\pm$  between members of the family and the action of  $\mathbf{F}$  thereon are again given by (2.22). The invariant  $I_4 = (\mathbf{CM}) \cdot \mathbf{M}$  is as in (2.1)<sub>2</sub>, but with  $\mathbf{M}$  now defined by (3.1)<sub>1</sub>, while the invariants  $I^\pm$  and the quantities  $I_8^\pm$  are again given by (2.23). The Cauchy stress tensor  $\sigma$  has the same form (2.24) as in three dimensions but is now restricted to two dimensions.

#### (a) Simple shear

For simple shear in the  $\mathbf{E}_1$  direction in the considered plane, the deformation gradient is given by  $\mathbf{F} = \mathbf{I} + \gamma \mathbf{E}_1 \otimes \mathbf{E}_2$ , where  $\gamma$  is the amount of shear. It follows that

$$\mathbf{FM} = \mathbf{M} + \gamma \sin \alpha \mathbf{E}_1 \quad \text{and} \quad \mathbf{FN} = \mathbf{N} + \gamma \cos \alpha \mathbf{E}_1. \quad (3.2)$$



The invariant  $I_4 = (\mathbf{CM}) \cdot \mathbf{M}$  is

$$I_4 = 1 + \gamma \sin 2\alpha + \gamma^2 \sin^2 \alpha, \quad (3.3)$$

while the required expressions  $(\mathbf{CN}) \cdot \mathbf{N}$  and  $(\mathbf{CM}) \cdot \mathbf{N}$  are given by

$$(\mathbf{CN}) \cdot \mathbf{N} = 1 - \gamma \sin 2\alpha + \gamma^2 \cos^2 \alpha \quad \text{and} \quad (\mathbf{CM}) \cdot \mathbf{N} = \gamma \cos 2\alpha + \gamma^2 \sin \alpha \cos \alpha. \quad (3.4)$$

On substitution of (3.4) into (2.23), we obtain

$$I^\pm = 1 + \gamma \sin 2(\alpha \pm \alpha_0) + \gamma^2 \sin^2(\alpha \pm \alpha_0) \quad (3.5)$$

and

$$I_8^\pm = \pm c_0 + \gamma \sin(\alpha_0 \pm 2\alpha) + \gamma^2 \sin \alpha \sin(\alpha_0 \pm \alpha). \quad (3.6)$$

From (2.24), the components of the Cauchy stress can be obtained, but we only need here the shear component  $\sigma_{12}$ , i.e.

$$\begin{aligned} \sigma_{12} = & 2\psi_1\gamma + 2[\psi_4 + c_0^2(\psi_{I^+} + \psi_{I^-}) + c_0(\psi_{8^+} - \psi_{8^-})]s(c + \gamma s) \\ & s_0[2c_0(\psi_{I^+} - \psi_{I^-}) + \psi_{8^+} + \psi_{8^-}](c^2 - s^2 + 2\gamma sc) \\ & + 2s_0^2(\psi_{I^+} + \psi_{I^-})c(\gamma c - s) \equiv \frac{\partial \Psi}{\partial \gamma}, \end{aligned} \quad (3.7)$$

where for conciseness we have written  $s = \sin \alpha$  and  $c = \cos \alpha$ .

For illustrative purposes, we now consider the model strain-energy function [13]

$$\begin{aligned} \Psi = & \frac{1}{2}\mu(I_1 - 3) + \eta \frac{k_1}{2k_2} \{\exp[k_2(I_4 - 1)^2] - 1\} + \frac{1}{2}v(I^+ - 1)^2 + \frac{1}{2}v(I^- - 1)^2 \\ & + \frac{1}{2}\kappa(I_8^+ - c_0)^2 + \frac{1}{2}\kappa(I_8^- + c_0)^2, \end{aligned} \quad (3.8)$$

which generalizes equation (2.34) to the case in which  $I^+ \neq I^-$  and  $I_8^+ \neq -I_8^-$ . With (2.25) it follows that

$$\psi_{I^+} + \psi_{I^-} = 2v\gamma[2sc(c_0^2 - s_0^2) + \gamma(s_0^2c^2 + s^2c_0^2)], \quad (3.9)$$

$$\psi_{I^+} - \psi_{I^-} = 4v\gamma s_0 c_0 (c^2 - s^2 + \gamma sc), \quad (3.10)$$

$$\psi_{8^+} + \psi_{8^-} = 2\kappa\gamma s_0 (c^2 - s^2 + \gamma sc) \quad (3.11)$$

and

$$\psi_{8^+} - \psi_{8^-} = 2\kappa\gamma s_0 c_0 (2c + \gamma s). \quad (3.12)$$

In this case, from (2.12), we obtain, with the help of (2.15)<sub>2</sub> and (3.3),

$$\eta = \exp \left[ -\frac{k_1}{2mk_2} \left\{ \exp[k_2\gamma^2 s^2 (\gamma s + 2c)^2] - \exp[k_2\gamma_c^2 s^2 (\gamma_c s + 2c)^2] \right\} \right], \quad (3.13)$$

where  $\gamma_c$  is the critical value of  $\gamma$  at which damage is initiated.

Hence, from (3.7), we obtain with (2.3) and (3.9)–(3.12)

$$\begin{aligned} \sigma_{12} = & \mu\gamma + 2\eta k_1 \exp[k_2\gamma^2 s^2 (2c + \gamma s)^2] s^2 (c + \gamma s) (2c + \gamma s) \gamma \\ & + 4v\gamma \{2s^2 c^2 (c_0^2 - s_0^2) + 2s_0^2 c_0^2 (c^2 - s^2)\} \\ & + 3sc\gamma [(c_0^2 - s_0^2)(c_0^2 s^2 + s_0^2 c^2) + 2s_0^2 c_0^2 (c^2 - s^2)] + \gamma^2 [(c_0^2 s^2 + s_0^2 c^2)^2 + 4s_0^2 c_0^2 s^2 c^2] \\ & + 2\kappa\gamma \{s_0^2 + 4s^2 c^2 (c_0^2 - s_0^2) + 3sc\gamma [(s_0^2 c^2 + s^2 c_0^2) + s^2 (c_0^2 - s_0^2)] + 2\gamma^2 s^2 (s_0^2 c^2 + s^2 c_0^2)\}. \end{aligned} \quad (3.14)$$

In figure 6, we plot the dimensionless shear stress  $\bar{\sigma}_{12} = \sigma_{12}/\mu$  from (3.14) against the amount of shear  $\gamma$  in order to illustrate the dependence on the various parameters. The specific parameter values used are  $\bar{k}_1 = k_1/\mu = 2$ ,  $\alpha = \pi/3$ ,  $k_2 = 0.1$ ,  $\gamma_c = 0.7$ ,  $m/\mu = 10$ ,  $\alpha_0 = \pi/5$ , and  $\bar{v} = v/\mu = 0.5, 2, \bar{\kappa} = \kappa/\mu = 0.6$ . Without cross-links  $\bar{v} = \bar{\kappa} = 0$ . Clearly, the shear stress response stiffens with an increase in the cross-link parameter  $\bar{v}$  without damage, while when damage is included the shear stress is reduced after a critical value of  $\gamma$  and can reach a maximum as  $\gamma$  increases, as

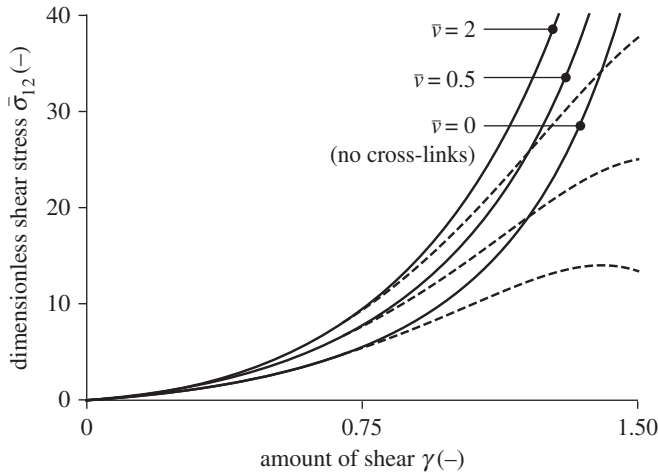


**Figure 6.** Plots of the dimensionless shear stress  $\bar{\sigma}_{12}$  versus the amount of shear  $\gamma$  with and without fibre damage (dashed and solid curves, respectively), with ( $\bar{\nu} = \nu/\mu = 0.5, 2, \bar{\kappa} = \kappa/\mu = 0.6$ ) and without ( $\bar{\nu} = \bar{\kappa} = 0$ ) cross-links. Parameter values:  $\bar{k}_1 = k_1/\mu = 2, \alpha = \pi/3, k_2 = 0.1, \gamma_c = 0.7, m/\mu = 10, \alpha_0 = \pi/5$ .

evidenced in the case when there are no cross-links. For the related elasticity tensor of model (3.8), which is relatively simple, we refer to appendix A.

#### 4. Discussion and concluding remarks

This study proposes a simple mechanical model for the damage progression of stretched collagen fibres based on a pseudoelastic approach. The model is used to fit the limited data that are available on the stretching of an individual collagen fibre, and the agreement with the data is very satisfactory. The model has then been used for the construction of a constitutive model for fibre-reinforced soft tissues in which the collagen fibres are supported by cross-links. The predictions of the model have been illustrated by an application to a simple shear test in which both damage and cross-links are accounted for. The related elasticity tensor is also provided with a view to analysing more complex boundary-value problems requiring a finite-element implementation.

To inform the further development of models that incorporate damage and cross-linking more data are needed on the response and damage of stretched single fibres, their influence on aggregates of collagen fibres embedded in tissues and also the mechanical properties of the cross-links. It is well known that the proportion of cross-links increases with age and causes a stiffening of the tissue [16]. In addition, several studies have shown that the stiffening of fibrous tissues is related to the concentration of cross-links (e.g. [17,18]). Such a relationship is captured by our model.

The effect of proteoglycans is essentially incorporated into the isotropic part of the tissue model, partly because it is still unclear what their mechanical contribution is to the overall response of the tissue. However, there is evidence that proteoglycans can support forces in the piconewton range when stretched [19], but it is not clear if the level of stresses they can support is relevant for a constitutive model of the type proposed in this paper. The review article by Scott [20] has described a mechanism between the collagen fibrils (as distinct from fibres) governed mainly by proteoglycans, which are essentially orthogonal to the fibrils (note that the author calls this complex an ‘elastic shape module’). However, it seems that there is no quantification yet available that shows how the force is transmitted between the individual fibrils. In the present paper, we focus on the collagen fibre level without accounting for the structure of fibrils and proteoglycans. In addition, because of the orthogonal arrangement of the proteoglycans with respect to the fibrils (see [21]), the force transition would only be relevant for rather large deformations. It is worth

pointing out, however, that force transition between proteoglycans and fibrils was accounted for in a mechanical model in [22], in which a collagen fibre is represented as a bundle of collagen fibrils cross-linked by proteoglycans.

More advanced multi-scale models are needed that capture the behaviours of the individual constituents such as proteoglycans, cross-linking proteins and their interaction with collagen molecules, fibrils and fibres and their aggregated contributions to the tissue. There is hope that current imaging modalities will allow a better understanding of the structure down to the nanoscale, but there is also a need for mechanical information at the same level. In order to tackle organ-level simulations the proposed model allows for a straightforward implementation within the finite-element method, which is a powerful tool for analysing more clinically relevant problems in health and disease.

**Data accessibility.** This article has no additional data.

**Authors' contributions.** G.A.H. and R.W.O. conceived and designed the research, interpreted the results and drafted the manuscript. Both authors edited and revised the manuscript, and gave final approval for publication.

**Competing interests.** We declare we have no competing interest.

**Funding.** The work of R.W.O. was funded in part by UK EPSRC grant no. EP/N014642/1.

**Acknowledgements.** The work of G.A.H. was partly supported by the Lead Project on 'Mechanics, Modeling and Simulation of Aortic Dissection', granted by Graz University of Technology, Austria.

## Appendix A

Here, we explicitly present the elasticity tensor  $\mathbb{C}$  in the material description, which is defined by

$$\mathbb{C} = 4 \frac{\partial^2 \Psi}{\partial \mathbf{C} \partial \mathbf{C}}. \quad (\text{A } 1)$$

Consider an energy function of the form  $\Psi(I_1, I_4, I^\pm, I_8^\pm, \eta)$ , where the four invariants are defined according to (2.1) and (2.23),  $\eta = \eta(I_4)$  is a damage variable accommodating damage only in the fibres, which is not specified explicitly at this point, and where  $I_4$  is the square of the stretch in the fibre direction. Then the derivatives of the invariants and  $\eta$  with respect to  $\mathbf{C}$  are

$$\frac{\partial I_1}{\partial \mathbf{C}} = \mathbf{I}, \quad \frac{\partial I_4}{\partial \mathbf{C}} = \mathbf{A}_M, \quad \frac{\partial I^\pm}{\partial \mathbf{C}} = c_0^2 \mathbf{A}_M \pm 2s_0 c_0 \mathbf{A}_{MN} + s_0^2 \mathbf{A}_N, \quad \frac{\partial I_8^\pm}{\partial \mathbf{C}} = \pm c_0 \mathbf{A}_M + s_0 \mathbf{A}_{MN}$$

and

$$\frac{\partial \eta}{\partial \mathbf{C}} = \eta'(I_4) \mathbf{A}_M,$$

where we have introduced the notations

$$\mathbf{A}_M = \mathbf{M} \otimes \mathbf{M}, \quad \mathbf{A}_{MN} = \frac{1}{2}(\mathbf{M} \otimes \mathbf{N} + \mathbf{N} \otimes \mathbf{M}) = \mathbf{A}_{NM}, \quad \mathbf{A}_N = \mathbf{N} \otimes \mathbf{N}.$$

It follows that

$$\begin{aligned} \frac{\partial \Psi}{\partial \mathbf{C}} &= \psi_1 \mathbf{I} + [\psi_4 + c_0^2(\psi_{I^+} + \psi_{I^-}) + c_0(\psi_{I_8^+} - \psi_{I_8^-}) + \psi_\eta \eta'] \mathbf{A}_M \\ &\quad + [2s_0 c_0(\psi_{I^+} - \psi_{I^-}) + s_0(\psi_{I_8^+} + \psi_{I_8^-})] \mathbf{A}_{MN} + s_0^2(\psi_{I^+} + \psi_{I^-}) \mathbf{A}_N, \end{aligned}$$

where we have used the abbreviations (2.3), (2.25) and  $\psi_\eta = \partial \Psi / \partial \eta$ . Then, we can write

$$\begin{aligned} \frac{\partial^2 \Psi}{\partial \mathbf{C} \partial \mathbf{C}} &= a_1 \mathbf{I} \otimes \mathbf{I} + a_2 (\mathbf{I} \otimes \mathbf{A}_M + \mathbf{A}_M \otimes \mathbf{I}) + a_3 \mathbf{A}_M \otimes \mathbf{A}_M + a_4 (\mathbf{I} \otimes \mathbf{A}_N + \mathbf{A}_N \otimes \mathbf{I}) \\ &\quad + a_5 (\mathbf{I} \otimes \mathbf{A}_{MN} + \mathbf{A}_{MN} \otimes \mathbf{I}) + a_6 (\mathbf{A}_M \otimes \mathbf{A}_N + \mathbf{A}_N \otimes \mathbf{A}_M) + a_7 \mathbf{A}_N \otimes \mathbf{A}_N \\ &\quad + a_8 (\mathbf{A}_M \otimes \mathbf{A}_{MN} + \mathbf{A}_{MN} \otimes \mathbf{A}_M) + a_9 (\mathbf{A}_N \otimes \mathbf{A}_{MN} + \mathbf{A}_{MN} \otimes \mathbf{A}_N) + a_{10} \mathbf{A}_{MN} \otimes \mathbf{A}_{MN}, \end{aligned}$$

where

$$\begin{aligned}
 a_1 &= \psi_{11}, \quad a_2 = \psi_{14} + \psi_{1\eta}\eta' + c_0^2(\psi_{1I^+} + \psi_{1I^-}) + c_0(\psi_{1I_8^+} - \psi_{1I_8^-}), \\
 a_3 &= \psi_{44} + 2\psi_{4\eta}\eta' + \psi_{\eta\eta}\eta'^2 + \psi_{\eta\eta''} + 2c_0^2[\psi_{4I^+} + \psi_{4I^-} + \eta'(\psi_{\eta I^+} + \psi_{\eta I^-})] \\
 &\quad + 2c_0[\psi_{4I_8^+} - \psi_{4I_8^-} + \eta'(\psi_{\eta I_8^+} - \psi_{\eta I_8^-})] + c_0^4(\psi_{I^+I^+} + \psi_{I^-I^-} + 2\psi_{I^+I^-}) \\
 &\quad + c_0^2(\psi_{I_8^+I_8^+} + \psi_{I_8^-I_8^-} - 2\psi_{I_8^+I_8^-}) + 2c_0^3(\psi_{I^+I_8^+} - \psi_{I^+I_8^-} + \psi_{I^-I_8^+} - \psi_{I^-I_8^-}), \\
 a_4 &= s_0^2(\psi_{1I^+} + \psi_{1I^-}), \quad a_5 = 2s_0c_0(\psi_{1I^+} - \psi_{1I^-}) + s_0(\psi_{1I_8^+} + \psi_{1I_8^-}), \\
 a_6 &= s_0^2[\psi_{4I^+} + \psi_{4I^-} + \eta'(\psi_{\eta I^+} + \psi_{\eta I^-})] + s_0^2c_0^2(\psi_{I^+I^+} + \psi_{I^-I^-} + 2\psi_{I^+I^-}) \\
 &\quad + s_0^2c_0(\psi_{I^+I_8^+} - \psi_{I^+I_8^-} + \psi_{I^-I_8^+} - \psi_{I^-I_8^-}), \\
 a_7 &= s_0^4(\psi_{I^+I^+} + \psi_{I^-I^-} + 2\psi_{I^+I^-}), \\
 a_8 &= 2s_0c_0[\psi_{4I^+} - \psi_{4I^-} + \eta'(\psi_{\eta I^+} - \psi_{\eta I^-})] + s_0[\psi_{4I_8^+} + \psi_{4I_8^-} + \eta'(\psi_{\eta I_8^+} + \psi_{\eta I_8^-})] \\
 &\quad + 2s_0c_0^3(\psi_{I^+I^+} - \psi_{I^-I^-}) + s_0c_0(\psi_{I_8^+I_8^+} - \psi_{I_8^-I_8^-}) \\
 &\quad + s_0c_0^2(3\psi_{I^+I_8^+} - \psi_{I^+I_8^-} - \psi_{I^-I_8^+} + 3\psi_{I^-I_8^-}), \\
 a_9 &= 2s_0^3c_0(\psi_{I^+I^+} - \psi_{I^-I^-}) + s_0^3(\psi_{I^+I_8^+} + \psi_{I^+I_8^-} + \psi_{I^-I_8^+} + \psi_{I^-I_8^-}) \\
 \text{and} \quad a_{10} &= 4s_0^2c_0^2(\psi_{I^+I^+} + \psi_{I^-I^-} - 2\psi_{I^+I^-}) + s_0^2(\psi_{I_8^+I_8^+} + \psi_{I_8^-I_8^-} + 2\psi_{I_8^+I_8^-}) \\
 &\quad + 4s_0^2c_0(\psi_{I^+I_8^+} + \psi_{I^+I_8^-} - \psi_{I^-I_8^+} - \psi_{I^-I_8^-}).
 \end{aligned}$$

For notational simplicity, the subscripts 1, 4,  $8^+$  and  $8^-$  on  $\psi$  stand for  $I_1, I_4, I_8^+$  and  $I_8^-$ , respectively, and we have introduced the abbreviation  $\psi_{\bullet\star} = \partial^2\Psi/\partial(\bullet)\partial(\star)$ . Note that in the expression for  $a_2$  in eqn (78) of [13] the sign before  $\psi_{1I_8^-}$  was incorrectly written as +.

For the model (3.8), these expressions simplify considerably, giving

$$a_1 = a_2 = a_4 = a_5 = a_8 = a_9 = 0$$

and

$$a_3 = \eta(\psi_{ff} - \psi_f^2/m) + 2\nu c_0^4 + 2\kappa c_0^2, \quad a_6 = 2\nu s_0^2 c_0^2, \quad a_7 = 2\nu s_0^4, \quad a_{10} = 8\nu s_0^2 c_0^2 + 2\kappa s_0^2,$$

where  $\psi_f$  is defined according to (2.7)<sub>2</sub> and  $\psi_{ff} = \partial^2\Psi_{\text{fib}}/\partial I_4^2$ . Note that the explicit expressions for  $\eta$  and  $\Psi_{\text{fib}}$  are provided in (2.12) and (2.15)<sub>2</sub>, respectively.

## References

1. Fratzl P (ed.) 2008 *Collagen. Structure and mechanics*. New York, NY: Springer.
2. Holzapfel GA, Ogden RW. 2010 Constitutive modelling of arteries. *Proc. R. Soc. A* **466**, 1551–1597. (doi:10.1098/rspa.2010.0058)
3. Holzapfel GA, Ogden RW. 2015 On the tension–compression switch in soft fibrous solids. *Eur. J. Mech. A/Solids* **49**, 561–569. (doi:10.1016/j.euromechsol.2014.09.005)
4. Holzapfel GA, Ogden RW. 2018 Biomechanical relevance of the microstructure in artery walls with a focus on passive and active components. *Am. J. Physiol. Heart Circ. Physiol.* **315**, H540–H549. (doi:10.1152/ajpheart.00117.2018)
5. Holzapfel GA, Ogden RW, Sherifova S. 2019 On fibre dispersion modelling of soft biological tissues: a review. *Proc. R. Soc. A* **475**, 20180736. (doi:10.1098/rspa.2018.0736)
6. Pins GD, Silver FH. 1995 A self-assembled collagen scaffold suitable for use in soft and hard tissue replacement. *Mater. Sci. Eng. C* **3**, 101–107. (doi:10.1016/0928-4931(95)00109-3)
7. Holzapfel GA, Fereidoonzhad B. 2017 Modeling of damage in soft biological tissues. In *Biomechanics of living organs. Hyperelastic constitutive laws for finite element modeling* (eds Y Payan, J Ohayon), pp. 101–123. New York, NY: Academic Press.
8. Hurschler C, Loitz-Ramage B, Vanderby Jr R. 1997 A structurally based stress-stretch relationship for tendon and ligament. *J. Biomech. Eng.* **119**, 392–399. (doi:10.1115/1.2798284)

9. Alastrué V, Rodríguez JF, Calvo B, Doblaré M. 2007 Structural damage models for fibrous biological soft tissues. *Int. J. Solids Struct.* **44**, 5894–5911. (doi:10.1016/j.ijsolstr.2007.02.004)
10. Hamedzadeh A, Gasser TC, Federico S. 2018 On the constitutive modelling of recruitment and damage of collagen fibres in soft biological tissues. *Eur. J. Mech. A/Solids* **72**, 483–496. (doi:10.1016/j.euromechsol.2018.04.007)
11. Lin WJ, Iafrati MD, Peattie RA, Dorfmann L. 2018 Growth and remodeling with application to abdominal aortic aneurysms. *J. Eng. Math.* **109**, 113–137. (doi:10.1007/s10665-017-9915-9)
12. Humphrey JD, Rajagopal KR. 2002 A constrained mixture model for growth and remodeling of soft tissues. *Math. Model. Methods Appl. Sci.* **12**, 407–430. (doi:10.1142/S0218202502001714)
13. Holzapfel GA, Ogden RW. 2020 An arterial constitutive model accounting for collagen content and cross-linking. *J. Mech. Phys. Solids* **136**, 103682. (doi:10.1016/j.jmps.2019.103682)
14. Ogden RW, Roxburgh DG. 1999 A pseudo-elastic model for the Mullins effect in filled rubber. *Proc. R. Soc. Lond. A* **455**, 2861–2877. (doi:10.1098/rspa.1999.0431)
15. Holzapfel GA. 2000 *Nonlinear solid mechanics. A continuum approach for engineering*. Chichester, UK: John Wiley & Sons.
16. Tsamis A, Krawiec JT, Vorp DA. 2013 Elastin and collagen fibre microstructure of the human aorta in ageing and disease: a review. *J. R. Soc. Interface* **10**, 20121004. (doi:10.1098/rsif.2012.1004)
17. Barodka VM, Joshi BL, Berkowitz DE, Hogue Jr CW, Nyhan D. 2011 Implications of vascular aging. *Anesth. Analg.* **112**, 1048–1060. (doi:10.1213/ANE.0b013e3182147e3c)
18. Cantini C, Kieffer P, Corman B, Limiñana P, Atkinson J, Lartaud-Idjouadiene I. 2001 Aminoguanidine and aortic wall mechanics, structure, and composition in aged rats. *Hypertension* **38**, 943–948. (doi:10.1161/hy1001.096211)
19. Haverkamp RG, Williams MA, Scott JE. 2005 Stretching single molecules of connective tissue glycans to characterize their shape-maintaining elasticity. *Biomacromolecules* **6**, 1816–1818. (doi:10.1021/bm0500392)
20. Scott JE. 2003 Elasticity in extracellular matrix ‘shape modules’ of tendon, cartilage, etc. A sliding proteoglycan-filament model. *J. Physiol.* **553**, 335–343. (doi:10.1113/jphysiol.2003.050179)
21. Scott JE. 2008 Cartilage is held together by elastic glycan strings. Physiological and pathological implications. *Biorheology* **45**, 209–217. (doi:10.3233/BIR-2008-0477)
22. Gasser TC. 2011 An irreversible constitutive model for fibrous soft biological tissue: a 3-D microfiber approach with demonstrative application to abdominal aortic aneurysms. *Acta Biomater.* **7**, 2457–2466. (doi:10.1016/j.actbio.2011.02.015)